

Dielectric Relaxation of Styrene-Isoprene Diblock Copolymer Solutions: A Common Solvent System

Ming-Long Yao, Hiroshi Watanabe, Keiichi Adachi, and Tadao Kotaka*

Department of Macromolecular Science, Faculty of Science, Osaka University, Toyonaka, Osaka 560, Japan

Received August 16, 1991; Revised Manuscript Received December 3, 1991

ABSTRACT: A dielectric study was carried out on solutions of polystyrene-*cis*-polyisoprene (SI) diblock copolymers in a common good solvent, toluene (TL). The I-blocks exhibited dielectric relaxation at long time scales due to fluctuation of their end-to-end vectors because of their dipoles along their contour. In concentrated solutions and/or at low temperatures, strong influences of microphase separation prevailed over such relaxations, reflecting the soft and deformable interphase between the S- and I-phases and a rather high mobility of the S-I junctions. These microphase-separated solutions exhibited dielectric loss (ϵ'') curves with two broad peaks at high and low frequencies. The former may be attributed to fluctuation of the S-I junctions within the interphase, and the latter, to fluctuation of the free I ends. For homogeneous SI/TL solutions at low SI concentrations and/or at high temperatures, ϵ'' curves with a sharp single peak were found. Their ϵ'' curves were compared with the prediction of the Stockmayer-Kennedy model for a Rouse chain composed of two chains having a different spring constant and friction factor. A reasonable agreement was found between the data and model prediction.

I. Introduction

In our previous papers, we discussed the dielectric behavior of polystyrene-*cis*-polyisoprene (SI) diblock copolymers in bulk¹ and in solution of an I-selective solvent, *n*-tetradecane (C14).² These systems are good models for examining through dielectric spectroscopy the dynamics of densely populated tethered chains confined in block copolymer microdomains. The morphology of such a microphase-separated structure is determined primarily as a function of the block copolymer architecture and solvent distribution, if any is present.^{3,4} In these particular systems, the rubbery I-blocks tightly bound to the surface of the glassy S-domains possess dipoles aligned in the same direction parallel along their chain contour and thus exhibit slow dielectric relaxation due to their global motion, or more specifically, due to their end-to-end vector fluctuation.⁵⁻⁷ This type of dielectric relaxation has been referred to as the dielectric *normal-mode* relaxation.⁶

In our previous work on bulk SI systems of nearly 50/50 S/I composition that formed an alternating lamellar structure composed of glassy S- and rubbery I-lamellae,¹ we found that the dielectric normal-mode relaxation of the I-blocks exhibits much longer relaxation times and a much broader mode distribution, as compared to bulk homo-*cis*-polyisoprene (PI) systems.^{6,7} This unique behavior of the I-blocks was attributed to the two types of confinements: thermodynamic confinement to maintain the uniform I-segment density profile throughout the lamellae of densely populated tethered I-block chains under the influence of spatial confinement within the lamellae. These two confinements are obviously interdependent and mutually enhancing for the I-block chains with one end fixed on the rigid S-domains.

Dilution of the bulk SI-systems, for example with C14, tends to release the two confinements.² The solvent C14 goes almost exclusively into the I-phase and thus provides more space for the I-blocks to ease the spatial confinement. Also the dilution with C14 increases the osmotic compressibility in the I-phase to weaken the thermodynamic confinement acting on the tethered I-block chains. At high dilution, SI molecules form micelles with rigid S-cores on which I-chains are tightly anchored. Thus the I-block chains still preserve the nature of tethered chains

but under the greatly reduced influence of the two confinements. Upon further dilution of the micellar solution with C14, the dielectric normal-mode relaxation behavior of the I-block chains became close (but not quite) to that of homo-PI chains.^{2,6,7}

On dilution of these SI-systems with a common good solvent, for example, toluene (TL) that dissolves both S- and I-blocks equally well, we expect certain new features to emerge: The interface of the microdomains is no longer rigid and the S-I junction points acquire a considerable mobility. At low SI concentrations, on the other hand, the microdomains disappear and the solution becomes homogeneous.^{3,8,9}

From this point of view, we examined dielectric behavior of toluene (TL) solutions of SI-diblock copolymers. In this paper, we present the results, placing emphasis on examining the difference between the behavior of SI/TL and SI/C14 solutions in relation to the difference in the S-I junction mobility. We also discuss the behavior of homogeneous SI/TL solutions. In such solutions individual SI-molecules behave as a chain with a discontinuity in the dynamical features along the contour, in which the I-block portion alone exhibits dielectric normal-mode relaxation, as in the case of polybutadiene-*cis*-polyisoprene block copolymers.¹⁰

II. Experimental Section

Two anionically polymerized SI-diblock copolymers, SI(42-42) and SI(43-86), were used. For comparison, their precursor homo-PI samples, PI(42) and PI(86), and a styrene-butadiene (SB) diblock copolymer sample, SB(41-40), were also used. The details of the synthesis and characterization were described elsewhere,¹ and the characteristics of these samples are summarized in Table I. The code numbers represent the molecular weights of constituent blocks in the thousands.

Dielectric measurements were made on toluene (TL) solutions of these SI, SB, and PI samples. A spectral grade TL (Wako Chemicals) was used as received without further purification.

A transformer bridge (GR 1615A; General Radio) and a capacitance cell with a lid for liquid sample use were employed. The details of the apparatus were also described elsewhere.⁷

The test solutions were prepared in the following way. In each case a precisely weighed polymer sample was first dissolved in TL to make a homogeneous solution of ~3% in the capacitance cell. The lid of the cell was left open to allow the fraction of TL

Table I
Characteristics of Polymer Samples

| code | $10^{-3}M_w$ | M_w/M_n | PS content, % |
|-----------------------------------|--------------|-----------|---------------|
| SI-Diblock Copolymer ^a | | | |
| SI(42-42) | 84.0 | 1.06 | 49.4 |
| SI(43-86) | 129.0 | 1.06 | 33.3 |
| SB-Diblock Copolymer ^b | | | |
| SB(41-40) | 80.9 | 1.06 | 51.2 |
| PI Homopolymer ^a | | | |
| PI(42) | 42.0 | 1.06 | 0 |
| PI(86) | 86.0 | 1.06 | 0 |

^a cis:trans:vinyl \approx 75:20:5 for I. ^b cis:trans:vinyl \approx 40:50:10 for B.

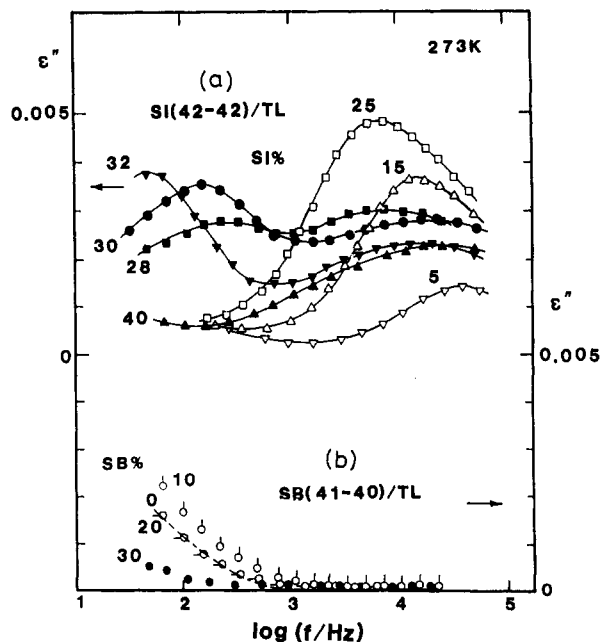


Figure 1. Frequency dependences of dielectric loss ϵ'' at 273 K for (a) SI(42-42)/TL and (b) SB(41-40)/TL solutions with concentrations as indicated. The dashed curve in part b indicates the ϵ'' curve for pure TL used.

to slowly evaporate. After closing the cell lid, the SI concentration c_{SI} was determined by weighing the whole cell containing the test solution just before the measurement.

On analyzing the dielectric data, we did not apply the frequency-temperature superposition procedure,¹¹ because the microphase-separated structure of SI/TL solutions was highly temperature sensitive.

III. Results and Discussion

III-1. Overview: Figure 1 shows the frequency f dependence of dielectric loss factors ϵ'' at 273 K for (a) SI(42-42)/TL and (b) SB(41-40)/TL solutions with concentrations c as indicated. For easy comparison, only the ϵ'' curves for representative c are shown. The dashed curve in part b indicates the ϵ'' curve of pure TL used.

In Figure 1a, we note that SI(42-42)/TL solutions have considerably large ϵ'' and exhibit significant dielectric relaxations. The features differ between those of $c_{SI} \leq 25\%$ (unfilled symbols) and of $c_{SI} \geq 28\%$ (filled ones). For $c_{SI} \leq 25\%$, the SI/TL solutions exhibit ϵ'' curves with a rather sharp single peak, and the peak location shifts to higher f with decreasing c_{SI} . On the other hand, for $c_{SI} \geq 28\%$, the solutions exhibit ϵ'' curves with double broad peaks. With increasing c_{SI} , the high- f peak shifts to higher frequencies and decreases in magnitude, whereas the low- f peak shifts to lower frequencies and increases in magnitude. For $c_{SI} = 40\%$, the low- f peak is outside ($f < 10$ Hz) our experimental window.

On the other hand, in Figure 1b for SB(41-40)/TL solutions, we note that the solutions have small ϵ'' and do not exhibit dielectric relaxation in the frequency range examined. The upswing of ϵ'' with decreasing $f < 10^3$ Hz is a result of direct current conduction due to ionic impurities in TL used, whose tendency is clearly seen in the dashed curve for pure TL. The tendency of a slight increase in ϵ'' at $f < 10^3$ Hz seen in Figure 1a for the 5% SI(42-42)/TL solution is also due to ionic impurities in TL.

As seen in Table I, the SI(42-42) and SB(41-40) copolymers have architecture close to each other. The molecular characteristics such as the characteristic ratio of the I- and B-blocks are nearly the same,² and also their segregation power toward the S-blocks and the solubility in TL are similar to each other. Thus the microdomain structures and motions of the diene chains should be almost the same in SI/TL and SB/TL solutions of the same c . However, the B-block chains have no dipoles parallel to their contour, and thus their global motion is dielectrically inert. Consequently, any dielectric relaxations observed only in SI/TL solutions but not observed in SB/TL solutions can be attributed to the global motion of the I-blocks. Similarly, any modes observed commonly in SI and SB solutions should be attributed to some other mechanisms. This was in fact the case in certain SI/C14 and SB/C14 solutions.² From this argument, we may assign both the single- and double-peak relaxation behaviors of the SI/TL solutions observed in Figure 1a to the *normal-mode relaxation* of the I-block chains reflecting their end-to-end vector fluctuation.

III-2. Effect of microphase separation: The drastic change in ϵ'' of the SI/TL solutions at a critical concentration c_{SI}^* around $\sim 25\%$ found in Figure 1a suggests that a structural change may have taken place at this concentration.

Sometime ago, Shibayama et al.⁸ made SAXS measurements on TL solutions of an SI copolymer with $M_I = M_S = 47 \times 10^3$, which was prepared via sequential anionic polymerization in benzene. They found that a critical concentration c_{SI}^* for formation of lamellae was between 19 and 23% at room temperature.⁸

We may say that their value of c_{SI}^* is in reasonably good agreement with ours, provided the following three factors are taken into account: First, their SAXS measurement was conducted at room temperature; second, the molecular weight of their sample was a number-averaged value and somewhat higher than ours; and third, their sample was polymerized in benzene so that the diene microstructure of the I-blocks might be somewhat different from ours polymerized in *n*-heptane,¹ although their literature⁸ did not provide the specific information.

More recently, Balsara et al.⁹ also made small-angle X-ray scattering (SAXS) measurements on SI(42-42)/TL solutions at 293–296 K. (Although the sample codes are not the same, their SI(43-41) sample⁹ was from the same source as our SI(42-42) sample.) They found that the solution was homogeneous at $c_{SI} \leq 13.3\%$ and a lamellar structure emerged at $c_{SI} \geq 24.5\%$.

The c_{SI}^* at 273 K determined here should be somewhat lower than that at room temperature. However, the SAXS-determined c_{SI}^* between 24.5 and 13.3 by Balsara et al. appears to be a little lower than the c_{SI}^* of 28–25% determined by us through the dielectric test. A possible explanation for this discrepancy is that the c_{SI}^* value could be different when the quantities of different nature were involved: A static structure was monitored in SAXS measurements, while a dynamic configuration of the I-

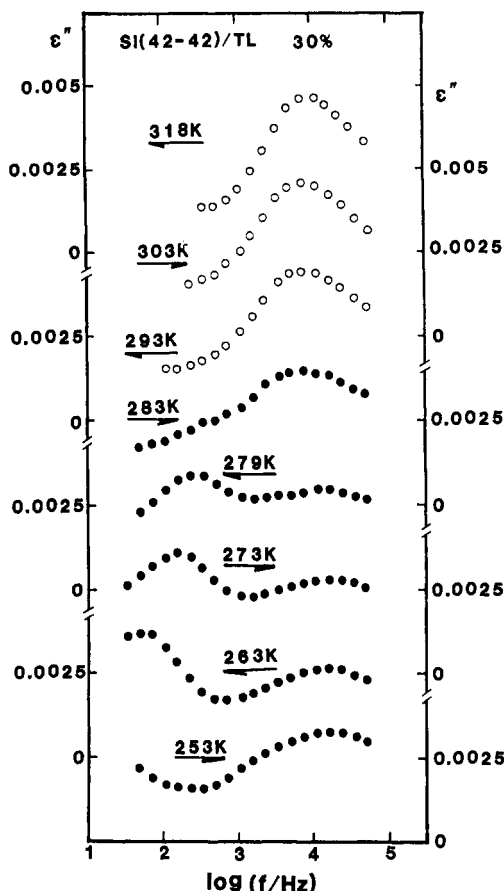


Figure 2. Comparison of the ϵ'' curves for the 30% SI(42-42)/TL solutions at various temperatures as indicated. The origins for the respective curves are shifted upward for easy comparison.

blocks was seen in the present dielectric measurements. From this point of view, the discrepancy found here seems to be justifiable. Thus we may conclude that the drastic change in the ϵ'' curves found in Figure 1a reflects the onset of microphase separation with increasing c_{SI} . The double-peaked ϵ'' curves for $c_{SI} \geq 28\%$ are due to the microdomain structure formed in TL, and the single-peaked ϵ'' curves for $c_{SI} \leq 25\%$ represent homogeneous solutions.

Figure 2 shows changes in the ϵ'' curves with temperature for SI(42-42)/TL with $c_{SI} = 30\%$. We note that the ϵ'' curves at $T \leq 283$ K (closed circles) exhibit double peaks, and those at $T \geq 293$ K (open circles), a single peak. This change is attributable to the heterogeneous-homogeneous (order-disorder) transition induced by heat.

From the peak frequencies f_m of the ϵ'' curves, we may evaluate dielectric relaxation times τ_n as

$$\tau_n = 1/(2\pi f_m) \quad (1)$$

However, we should hasten to add that the τ_n thus determined does not necessarily reflect the longest normal-mode relaxation time τ_1 for the fundamental mode, as opposed to the systems involving free homo-PI chains.^{6,7} The τ_n can be the τ_1 , only when the relaxation mode distribution or the shape of the ϵ'' curve conform either to the Debye (a single mode) type or to the Rouse model¹² or to the tube model,¹³ or any other models in which the fundamental mode dominates. Otherwise, the τ_n merely represents a complicated average of the relaxation times specific to the particular mode distribution.^{1,2} Thus, when the shape of the ϵ'' curve changes with concentration and/or temperature, a comparison of τ_n itself is meaningless.^{1,2}

Keeping the above precaution in mind, we attempted to examine the changes in the dielectric behavior of the

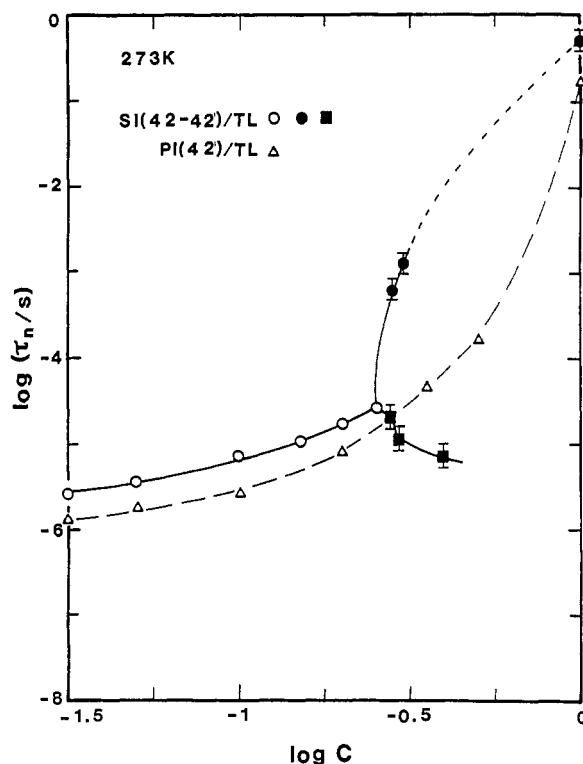


Figure 3. Concentration dependence of the dielectric relaxation time τ_n at 273 K for the SI(42-42)/TL solutions. The τ_n 's were evaluated from the location of the ϵ'' peaks with eq 1.

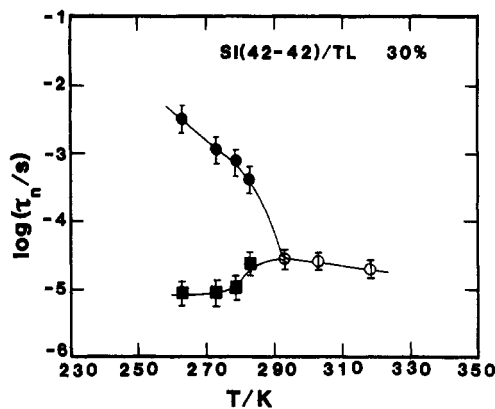


Figure 4. Temperature dependence of the dielectric relaxation time τ_n for the 30% SI(42-42)/TL solution. The τ_n 's were evaluated from the locations of the ϵ'' peaks with eq 1.

SI/TL solutions with concentration c_{SI} and temperature, both of which obviously influence the microdomain structure.

In Figure 1, we already saw that, for SI(42-42)/TL at $T = 273$ K, the ϵ'' curves exhibit double peaks for those with $c_{SI} \geq 28\%$, while the ϵ'' curves exhibit a single peak for those with $c_{SI} \leq 25\%$. On the other hand, we see in Figure 2 that, for SI(42-42)/TL with $c_{SI} = 30\%$ at $T \leq 283$ K, the ϵ'' curves exhibit double peaks, and for those at $T \geq 293$ K, a single peak. For the former, we estimated two τ_n , and for the latter, the single τ_n .

Figures 3 and 4 respectively show the dependence of τ_n on c_{SI} for SI(42-42)/TL at 273 K and on T for the same system with $c_{SI} = 30\%$. In Figure 3, we also plotted τ_n versus PI concentration c_{PI} for PI(42)/TL solutions at 273 K.

For such broad ϵ'' curves, the τ_n evaluated from eq 1 should be far shorter than the longest relaxation time τ_1 , as explained in the previous paper.² However, even such

τ_n 's are still sufficient for the following qualitative discussion on the nature of the double peaks in the broad ϵ'' curves.

As seen in Figure 3, for the solutions at 273 K with $c_{SI} \geq c_{SI}^*$ ($\approx 28\%$; in the phase-separated regime) the longer τ_n increases with a small increase in c_{SI} , while the shorter τ_n decreases. We have already seen in Figure 1a that, with increasing c_{SI} ($\geq c_{SI}^* \approx 28\%$), the high- f peak shifts to the higher f side and decreases its intensity, while the low- f ϵ'' peak shifts to the lower f side and increases intensity. A similar trend is seen in Figure 4 for the 30% solution at $T \leq 283$ K, for which the longer τ_n (filled circles) increases with decreasing T , while the shorter τ_n (filled squares) decreases. These results give a clue to interpret the unique double-peaked ϵ'' curves of the normal-mode relaxation in SI/TL solutions.

In the previous papers,^{1,2} we found that the ϵ'' curves are broad but still exhibit a single peak for microphase-separated SI/C14 solutions (in the range of f within our experimental window) as well as for the bulk SI systems. As explained earlier, the spatial and thermodynamic confinements may differ between these two systems, but the S-I junction points are fixed in space in both systems which commonly contain glassy S-domains.

On the other hand, in the present SI/TL solutions, the S-domains diluted with TL are no longer rigid but in a rubbery (or flow) state, thereby allowing the S-I junction points to move easily in the S-I interphase. Thus an I-block chain in the microphase-separated SI/TL solution has two nonequivalent movable ends (the S-I junction and the free end). The double-peak relaxation found in Figures 1 and 2 may be interpreted in the following way in relation to the motion of the junctions.

In such SI/TL solutions, the S-I junctions should be located on average at the center of the interphase but fluctuate with time. Such junction fluctuation should also induce fluctuation of the end-to-end vectors of the I-blocks. With increasing c_{SI} (or lowering T), the segregation power between I- and S-blocks becomes larger, leading to a narrower interphase and to a larger free-energy increment due to the junction fluctuation. This suggests that the restoring force on the S-I junctions to pull them back to their average location becomes larger with increasing c_{SI} . When this enhancement of the restoring force overwhelms the increase in the friction of the S-I junctions, the time constant for the junction-fluctuation mechanism becomes shorter with increasing c_{SI} and/or lowering T . In addition, the width of the interphase and thus the amplitude of the junction fluctuation should decrease with increasing c_{SI} and/or lowering T , leading to a decrease in the relaxation intensity. We may thus consider that the junction-fluctuation mechanism is responsible for the high- f ϵ'' peak of the microphase-separated SI/TL solutions.

At time scales longer than that for the junction fluctuation, the motion of the S-I junction points would be smeared and the junctions may now be fixed points located at their average positions in the S-I interphase. For such cases, fluctuation of the end-to-end vectors due to the motion of the free I-ends in the SI/TL systems would become essentially the same as those in bulk SI and SI/C14 systems. The dielectric relaxation due to the motion of the free I-ends in the SI/TL systems becomes slower and the intensity increases with increasing c_{SI} , as was the case for SI/C14 solutions. This explains the features of the low- f ϵ'' peak.

III-3. Behavior in a homogeneous state: As seen in Figures 1-4, the SI/TL solutions at low c_{SI} and/or at high T are in a homogeneous (disordered) state, exhibiting ϵ''

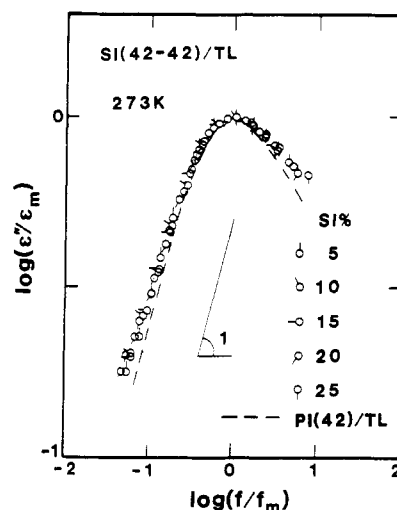


Figure 5. Comparison of the shape of the ϵ'' curves at 273 K for homogeneous SI(42-42)/TL solutions with c_{SI} as indicated. Direct current conductivities due to impurities involved in TL significantly contributed to ϵ'' of the SI/TL solutions of small c_{SI} at low f ($< 10^3$ Hz; cf. Figure 1), and the data points in that f range are not shown in the figure. The dashed curve indicates the ϵ'' curves for PI(42)/TL solutions with $c_{PI} \geq 3\%$.

curves with a single peak. Interestingly, as seen in Figure 3, in the homogeneous state the c_{SI} dependence of τ_n for SI(42-42)/TL and the c_{PI} dependence of τ_n for PI(42)/TL are parallel, and the former are about twice as large as the latter, reflecting difference in the dynamics of an isolated SI chain and of its precursor PI chain.

Then Figure 5 compares the shape of the ϵ'' curves reduced at the peaks for SI(42-42) and PI/TL solutions. The shape reflects the dielectric relaxation mode distribution, as explained in the previous paper.² For PI/TL solutions, the shape of the reduced ϵ''/ϵ_m vs f/f_m curves is insensitive to c_{PI} in the range of $c_{PI} \geq 3\%$ (as well as to the PI molecular weight), as shown in Figure 5 with the dashed curve. For SI(42-42)/TL solutions with $5 \leq c_{SI} (\%) \leq 25$, the reduced curves (circles) at 273 K also have nearly the same shape and are a little broader than those of the PI/TL solutions.

In these dilute TL solutions, the SI- or PI-chains are in a nonentangled regime. For such a PI-chain, the conventional Rouse model¹² may be applicable. On the other hand, for an SI-copolymer chain we have to consider differences in the characteristics of the I- and S-segments involved. The Rouse model was extended for such block copolymer chains by Hansen and Shen,¹⁴ Hall and De Wames,¹⁵ and Stockmayer and Kennedy.¹⁶ In the former two cases the equation of motion was formulated for a discrete block copolymer chain and in the last case for a continuous chain.

Here we apply the Stockmayer-Kennedy (SK) model¹⁶ to nonentangled SI/TL solutions. For an SI-chain with the parallel dipoles only along the I-block, the autocorrelation function for the dielectric normal-mode relaxation can be written as⁵⁻⁷

$$\Phi(t) = \frac{\langle \mathbf{R}_I(t) \cdot \mathbf{R}_I(0) \rangle}{\langle \mathbf{R}_I(0) \cdot \mathbf{R}_I(0) \rangle} \quad (2)$$

where $\mathbf{R}_I(t)$ is the end-to-end vector at time t of the I-block. The dielectric loss factor at frequency f is related to $\Phi(t)$ as⁵⁻⁷

$$\epsilon''(f) = -\Delta\epsilon \int_0^\infty (d\Phi(t)/dt) \sin 2\pi ft \, dt \quad (3)$$

with $\Delta\epsilon$ being the relaxation intensity. Thus, solving the

equation of motion of the SK-model, we can calculate $\langle \mathbf{R}_I(t) \cdot \mathbf{R}_I(0) \rangle$ and thus ϵ'' . In the SK-model, the Rouse equation holds within respective blocks, and the free-end conditions are used for the S- and I-ends as the boundary conditions.¹⁶ In addition, a connectivity and a force balance are required for the S-I junction point.

Prediction of the SK model: We here consider an SI-diblock copolymer chain composed of N_S S-segments and N_I I-segments connected with Gaussian springs. The segmental friction and spring constant for the J -block ($J = S$ or I) are denoted, respectively, by ζ_J and $\kappa_J = 3kT/b_J^2$, with b_J being the J -segment size. To apply the SK-model to our SI-block chains, we first need to decide the S- and I-segment sizes. Although the segment size for the bead-spring model is in general not uniquely determined, the model predictions for *slow* dynamic behavior do not depend on the choice of the segment size. Thus here we choose size b of the I- and S-segments to be the same so that their κ ($=3kT/b^2$) is the same. Then we have

$$N_I = M_I/m_I, \quad N_S = M_S/m_S, \quad b^2 = F_I m_I = F_S m_S \quad (4)$$

where m_J and M_J ($J = S$ or I) represent the molecular weights of the J -segment and the J -block as a whole, respectively, and F_J is the proportionality coefficient between b^2 and m_J for the J -segment.

With the above simplification for the segment size, the eigenvalue (β_p) equation of the SK-model becomes

$$-\lambda \tan \beta_p \lambda \theta = \tan \beta_p (1 - \theta) \quad p = 1, 2, \dots \quad (5)$$

with

$$\lambda = [\zeta_I/\zeta_S]^{1/2}, \quad \theta = N_I/[N_S + N_I] \quad (6)$$

The relaxation times τ_p^{SI} for the p th normal mode is written in terms of β_p as

$$\tau_p^{\text{SI}} = \zeta_S N^2 / \kappa \beta_p^2 \quad (7)$$

and ϵ'' as

$$\epsilon''_{\text{SI}} = Q \nu_{\text{SI}} (N_I + N_S) b^2 \sum_p g_p \frac{\omega \tau_p^{\text{SI}}}{1 + (\omega \tau_p^{\text{SI}})^2}, \quad \omega = 2\pi f \quad (8)$$

Here ν_{SI} ($\propto c_{\text{SI}}/M_{\text{SI}}$) is the number of SI-chains per unit volume, and Q is a proportionality constant. The intensity factor for the p th mode, g_p , is calculated from a Gaussian distribution function for bond vectors connecting neighboring segments as

$$g_p = (1/A_p) \cos^2 \beta_p (1 - \theta) \{1 - \cos \lambda \theta \beta_p\}^2 \quad (9)$$

with

$$A_p = (\beta_p^2/2) [\theta \lambda^2 \cos^2 \beta_p (1 - \theta) + (1 - \theta) \cos^2 \beta_p \theta] - (\beta_p/4) [\lambda \sin 2\beta_p \lambda \theta \cos^2 \beta_p (1 - \theta) + \sin 2\beta_p (1 - \theta) \cos^2 \beta_p \theta] \quad (10)$$

Model parameters: To make a quantitative comparison of the ϵ'' data and the model prediction, we need to determine the parameters involved in eqs 5–10. First, for a PI-chain composed of N_I segments, the SK-model leads to the well-known Rouse result

$$\epsilon''_{\text{PI}} = Q \nu_{\text{PI}} N_I b^2 \sum_p g_p \frac{\omega \tau_p^{\text{PI}}}{1 + (\omega \tau_p^{\text{PI}})^2}; \quad \tau_1^{\text{PI}} = \zeta_I N_I^2 / \kappa \pi^2$$

(for PI) $\tau_p^{\text{PI}} = p^{-2} \tau_1^{\text{PI}}; \quad p = 1, 3, 5, \dots$ (11)

Comparing ϵ'' given by eq 11 with the data for a PI/TL solution, we can evaluate Q and τ_p^{PI} . We here assume the

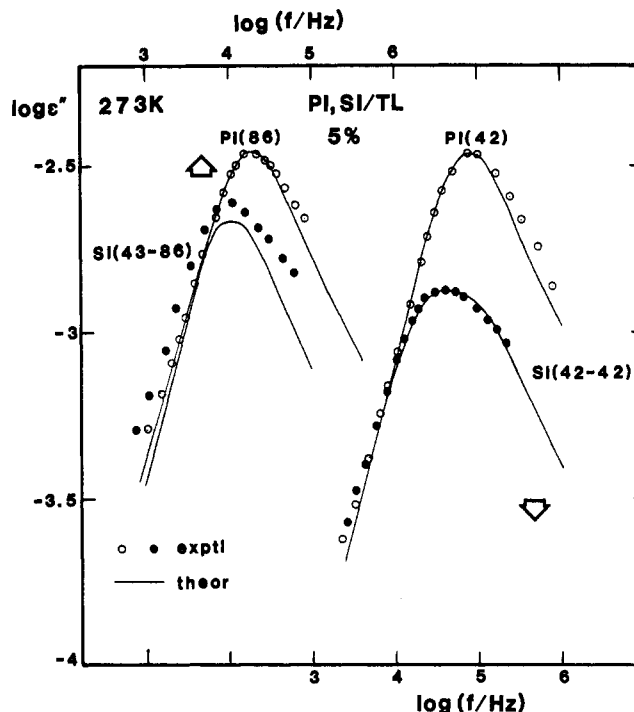


Figure 6. Comparison of the ϵ'' curves at 273 K for homogeneous TL solutions ($c = 5\%$) of the SI- and precursor PI-chains as indicated. The solid curves represent the predictions of the Stockmayer-Kennedy model with the parameters $m_I/m_S = 0.65$ and $\zeta_I/\zeta_S = 0.9$.

friction ζ_I of the I-segment to be nearly the same in our dilute SI/TL and PI/TL solutions of the same c . Then τ_p^{SI} of an SI-copolymer may be related to τ_1^{PI} of its precursor PI as (cf. eqs 7 and 11):

$$\tau_p^{\text{SI}} = (\pi/\beta_p \theta \lambda)^2 \tau_1^{\text{PI}} \quad (12)$$

Thus, once τ_1^{PI} and Q are experimentally determined for the precursor PI, we only need to estimate $\lambda = [\zeta_I/\zeta_S]^{1/2}$ and $\theta = N_I/(N_I + N_S)$ to describe ϵ'' of the SI-copolymer. (In other words, we do not need to estimate κ , ζ_I , ζ_S , N_I , and N_S separately, as seen from eqs 4–12.)

Because we have used a common κ for the I- and S-segments in the model, eq 4 holds for the segment molecular weights m_S and m_I . The m_I/m_S ratio ($=F_S/F_I$; cf. eq 4) is identical to the ratio of the mean-square end-to-end distances of the S- and I-blocks of the same molecular weight. We here approximate this ratio for our dilute TL solutions to be the same as the ratio at the infinite dilution. Then we can estimate m_I/m_S to be 0.65 by applying the Flory-Fox relation¹⁷ to the reported intrinsic viscosity data:¹⁸

$$[\eta] = 20.0 \times 10^{-3} M^{0.728} \text{ mL/g (for PI/TL)} \quad (13)$$

$$[\eta] = 10.5 \times 10^{-3} M^{0.73} \text{ mL/g (for PS/TL)} \quad (14)$$

From this m_I/m_S ratio and molecular weights M_I and M_S of the I- and S-blocks, we can estimate $\theta = N_I/[N_I + N_S] = M_I/[M_I + (m_I/m_S)M_S]$. Then the only unknown parameter is $\lambda = (\zeta_I/\zeta_S)^{1/2}$ that can be evaluated from a comparison of the calculated and observed ϵ'' curves for a particular SI/TL solution. We assume that ζ_I and ζ_S are common to different SI-copolymers in our dilute TL solutions (of the same c). Then the λ value determined for a particular SI/TL solution can be used for characters of other SI-copolymers (unless the molecular characteristics of the SIs are not very different).

Comparison of the data and model: Figure 6 shows

ϵ'' curves at 273 K for dilute TL solutions (with $c = 5\%$) of SI(42-42) and SI(43-86) and corresponding PI precursors. No phase separation took place in those systems. With adequate choice of τ_1^{PI} and Q values (cf. eq 11), we see that the ϵ'' data for PI(42)/TL at low f can be well described by eq 11 as indicated with the solid curve. Using the τ_1^{PI} and Q values thus evaluated, we compared the data for SI(42-42)/TL at 5% with the ϵ''_{SI} curve calculated from eq 8 and found that the ϵ''_{SI} curve with $\lambda^2 = \zeta_1/\zeta_S = 0.9$ (and $m_1/m_S = 0.65$) reasonably well describes the data, as seen in Figure 6. Using these parameter values, we can reasonably well describe the relation between the concentration dependence of τ_n 's of the SI/TL and PI/TL homogeneous solutions shown in Figure 3.

Thus, with these adequate choices of the parameter values, the SK-model can describe slow dielectric relaxations of the SI- and precursor PI-chains in a unified way.

We further compared in Figure 6 the model prediction and the data for SI(43-86)/TL and its precursor PI(86)/TL solutions, using the parameters determined for the TL solutions of SI(42-42) and PI(42). As shown in Figure 6 with the solid curve, agreement is fairly good for the SI(43-86) system, for which a difference of 20-30% is observed but the shape of the curve and the peak location are correctly predicted by the model.

Ambiguities still remain in the assumptions we made for the estimation of the model parameters. In addition, hydrodynamic interaction and excluded volume effect that are not accounted in the SK-model may not be negligible for our TL solutions. However, the results found in Figure 6 suggest in a semiquantitative sense the validity of the SK-model for describing slow dynamics of homogeneous block copolymer solutions.

IV. Conclusion

For solutions of SI-block copolymers in a common solvent, toluene (TL), we found strong influences of the microphase separation on the dielectric normal-mode relaxation of the I-blocks involved. In microphase-separated SI/TL solutions at high c_{SI} and/or low T , the

I-blocks exhibit broad double-peaked ϵ'' curves. In such solutions, the S-phase diluted with TL is liquid and the S-I junction points are movable. The high- f mode of the SI/TL solution is attributable to the fluctuation of such junctions in the S-I interphase, and the low- f mode, to the fluctuation of free I-ends.

A homogeneous SI/TL solution at low c_{SI} and/or at high T exhibits an ϵ'' curve with a rather sharp single peak. Such ϵ'' curves were compared with the prediction of the Stockmayer-Kennedy model that considers a Rouse chain having heterogeneity along its contour. Reasonable agreements were found between the data and model predictions.

References and Notes

- (1) Yao, M.-L.; Watanabe, H.; Adachi, K.; Kotaka, T. *Macromolecules* **1991**, *24*, 2955.
- (2) Yao, M.-L.; Watanabe, H.; Adachi, K.; Kotaka, T. *Macromolecules* **1991**, *24*, 6175.
- (3) Meier, D. J. *J. Polym. Sci.* **1969**, C26, 81.
- (4) Helfand, E.; Wasserman, Z. R. *Macromolecules* **1976**, *9*, 829; **1978**, *11*, 960.
- (5) Stockmayer, W. H. *Pure Appl. Chem.* **1969**, *15*, 539.
- (6) Adachi, K.; Kotaka, T. *Macromolecules* **1984**, *17*, 120; **1985**, *18*, 466.
- (7) Imanishi, Y.; Adachi, K.; Kotaka, T. *J. Chem. Phys.* **1988**, *89*, 7585.
- (8) Shibayama, M.; Hashimoto, T.; Hasegawa, H.; Kawai, H. *Macromolecules* **1983**, *16*, 1427.
- (9) Balsara, N. P.; Eastman, C. E.; Foster, M. D.; Lodge, T. P.; Tirrell, M. *Macromol. Chem., Macromol. Symp.* **1991**, *45*, 213.
- (10) Adachi, K.; Nishi, I.; Doi, H.; Kotaka, T. *Macromolecules* **1991**, *24*, 5843.
- (11) Ferry, J. D. *Viscoelastic Properties of Polymers*, 3rd ed.; John Wiley: New York, 1980.
- (12) Rouse, P. E. *J. Chem. Phys.* **1953**, *21*, 1272.
- (13) Doi, M.; Edwards, S. F. *The Theory of Polymer Dynamics*; Clarendon Press: Oxford, 1986.
- (14) Hansen, D. R.; Shen, M. *Macromolecules* **1975**, *8*, 343.
- (15) Hall, W. F.; De Wames, R. E. *Macromolecules* **1975**, *8*, 349.
- (16) Stockmayer, W. H.; Kennedy, J. W. *Macromolecules* **1975**, *8*, 351.
- (17) Flory, P. J. *Principles of Polymer Chemistry*; Cornell University Press: Ithaca, NY, 1953; Chapter 14.
- (18) Kurata, M.; Tsunashima, Y.; Iwama, M.; Kamada, K. In *Polymer Handbook*, 2nd ed.; Brundrup, J., Immergut, E. H., Eds.; John Wiley: New York, 1975; Chapter IV.